

Central Pseudorapidity Gaps in Events with a Leading Antiproton at the Fermilab Tevatron $\bar{p}p$ Collider

D. Acosta,¹⁴ T. Affolder,²⁵ H. Akimoto,⁵⁰ M. G. Albrow,¹³ D. Ambrose,³⁷ D. Amidei,²⁸ K. Anikeev,²⁷ J. Antos,¹ G. Apollinari,¹³ T. Arisawa,⁵⁰ A. Artikov,¹¹ T. Asakawa,⁴⁸ W. Ashmanskas,¹⁰ F. Azfar,³⁵ P. Azzi-Bacchetta,³⁶ N. Bacchetta,³⁶ H. Bachacou,²⁵ W. Badgett,¹³ S. Bailey,¹⁸ P. de Barbaro,⁴¹ A. Barbaro-Galtieri,²⁵ V. E. Barnes,⁴⁰ B. A. Barnett,²¹ S. Baroiant,⁵ M. Barone,¹⁵ G. Bauer,²⁷ F. Bedeschi,³⁸ S. Behari,²¹ S. Belforte,⁴⁷ W. H. Bell,¹⁷ G. Bellettini,³⁸ J. Bellinger,⁵¹ D. Benjamin,¹² J. Bensinger,⁴ A. Beretvas,¹³ J. Berryhill,¹⁰ A. Bhatti,⁴² M. Binkley,¹³ D. Bisello,³⁶ M. Bishai,¹³ R. E. Blair,² C. Blocker,⁴ K. Bloom,²⁸ B. Blumenfeld,²¹ S. R. Blusk,⁴¹ A. Bocci,⁴² A. Bodek,⁴¹ G. Bolla,⁴⁰ A. Bolshov,²⁷ Y. Bonushkin,⁶ D. Bortoletto,⁴⁰ J. Boudreau,³⁹ A. Brandl,³¹ C. Bromberg,²⁹ M. Brozovic,¹² E. Brubaker,²⁵ N. Bruner,³¹ J. Budagov,¹¹ H. S. Budd,⁴¹ K. Burkett,¹⁸ G. Busetto,³⁶ K. L. Byrum,² S. Cabrera,¹² P. Calafiura,²⁵ M. Campbell,²⁸ W. Carithers,²⁵ J. Carlson,²⁸ D. Carlsmith,⁵¹ W. Caskey,⁵ A. Castro,³ D. Cauz,⁴⁷ A. Cerri,³⁸ L. Cerrito,²⁰ A. W. Chan,¹ P. S. Chang,¹ P. T. Chang,¹ J. Chapman,²⁸ C. Chen,³⁷ Y. C. Chen,¹ M.-T. Cheng,¹ M. Chertok,⁵ G. Chiarelli,³⁸ I. Chirikov-Zorin,¹¹ G. Chlachidze,¹¹ F. Chlebana,¹³ L. Christofek,²⁰ M. L. Chu,¹ J. Y. Chung,³³ W.-H. Chung,⁵¹ Y. S. Chung,⁴¹ C. I. Ciobanu,³³ A. G. Clark,¹⁶ M. Coca,⁴¹ A. P. Colijn,¹³ A. Connolly,²⁵ M. Convery,⁴² J. Conway,⁴⁴ M. Cordelli,¹⁵ J. Cranshaw,⁴⁶ R. Culbertson,¹³ D. Dagenhart,⁴ S. D'Auria,¹⁷ S. De Cecco,⁴³ F. DeJongh,¹³ S. Dell'Agnello,¹⁵ M. Dell'Orso,³⁸ S. Demers,⁴¹ L. Demortier,⁴² M. Deninno,³ D. De Pedis,⁴³ P. F. Derwent,¹³ T. Devlin,⁴⁴ C. Dionisi,⁴³ J. R. Dittmann,¹³ A. Dominguez,²⁵ S. Donati,³⁸ M. D'Onofrio,³⁸ T. Dorigo,³⁶ N. Eddy,²⁰ K. Einsweiler,²⁵ E. Engels, Jr.,³⁹ R. Erbacher,¹³ D. Errede,²⁰ S. Errede,²⁰ R. Eusebi,⁴¹ Q. Fan,⁴¹ H.-C. Fang,²⁵ S. Farrington,¹⁷ R. G. Feild,⁵² J. P. Fernandez,⁴⁰ C. Ferretti,²⁸ R. D. Field,¹⁴ I. Fiori,³ B. Flaughner,¹³ L. R. Flores-Castillo,³⁹ G. W. Foster,¹³ M. Franklin,¹⁸ J. Freeman,¹³ J. Friedman,²⁷ Y. Fukui,²³ I. Furic,²⁷ S. Galeotti,³⁸ A. Gallas,³² M. Gallinaro,⁴² T. Gao,³⁷ M. Garcia-Sciveres,²⁵ A. F. Garfinkel,⁴⁰ P. Gatti,³⁶ C. Gay,⁵² D. W. Gerdes,²⁸ E. Gerstein,⁹ S. Giagu,⁴³ P. Giannetti,³⁸ K. Giolo,⁴⁰ M. Giordani,⁵ V. Glagolev,¹¹ D. Glenzinski,¹³ M. Gold,³¹ N. Goldschmidt,²⁸ J. Goldstein,¹³ G. Gomez,⁸ M. Goncharov,⁴⁵ I. Gorelov,³¹ A. T. Goshaw,¹² Y. Gotra,³⁹ K. Goulianos,⁴² C. Green,⁴⁰ A. Gresele,³⁶ G. Grim,⁵ C. Grosso-Pilcher,¹⁰ M. Guenther,⁴⁰ G. Guillian,²⁸ J. Guimaraes da Costa,¹⁸ R. M. Haas,¹⁴ C. Haber,²⁵ S. R. Hahn,¹³ E. Halkiadakis,⁴¹ C. Hall,¹⁸ T. Handa,¹⁹ R. Handler,⁵¹ F. Happacher,¹⁵ K. Hara,⁴⁸ A. D. Hardman,⁴⁰ R. M. Harris,¹³ F. Hartmann,²² K. Hatakeyama,⁴² J. Hauser,⁶ J. Heinrich,³⁷ A. Heiss,²² M. Henneke,²² M. Herndon,²¹ C. Hill,⁷ A. Hocker,⁴¹ K. D. Hoffman,¹⁰ R. Hollebeek,³⁷ L. Holloway,²⁰ S. Hou,¹ B. T. Huffman,³⁵ R. Hughes,³³ J. Huston,²⁹ J. Huth,¹⁸ H. Ikeda,⁴⁸ C. Issever,⁷ J. Incandela,⁷ G. Introzzi,³⁸ M. Iori,⁴³ A. Ivanov,⁴¹ J. Iwai,⁵⁰ Y. Iwata,¹⁹ B. Iyutin,²⁷ E. James,²⁸ M. Jones,³⁷ U. Joshi,¹³ H. Kambara,¹⁶ T. Kamon,⁴⁵ T. Kaneko,⁴⁸ J. Kang,²⁸ M. Karagoz Unel,³² K. Karr,⁴⁹ S. Kartal,¹³ H. Kasha,⁵² Y. Kato,³⁴ T. A. Keaffaber,⁴⁰ K. Kelley,²⁷ M. Kelly,²⁸ R. D. Kennedy,¹³ R. Kephart,¹³ D. Khazins,¹² T. Kikuchi,⁴⁸ B. Kilminster,⁴¹ B. J. Kim,²⁴ D. H. Kim,²⁴ H. S. Kim,²⁰ M. J. Kim,⁹ S. B. Kim,²⁴ S. H. Kim,⁴⁸ T. H. Kim,²⁷ Y. K. Kim,²⁵ M. Kirby,¹² M. Kirk,⁴ L. Kirsch,⁴ S. Klimenko,¹⁴ P. Koehn,³³ K. Kondo,⁵⁰ J. Konigsberg,¹⁴ A. Korn,²⁷ A. Korytov,¹⁴ K. Kotelnikov,³⁰ E. Kovacs,² J. Kroll,³⁷ M. Kruse,¹² V. Krutelyov,⁴⁵ S. E. Kuhlmann,² K. Kurino,¹⁹ T. Kuwabara,⁴⁸ N. Kuznetsova,¹³ A. T. Laasanen,⁴⁰ N. Lai,¹⁰ S. Lami,⁴² S. Lammel,¹³ J. Lancaster,¹² K. Lannon,²⁰ M. Lancaster,²⁶ R. Lander,⁵ A. Lath,⁴⁴ G. Latino,³¹ T. LeCompte,² Y. Le,²¹ J. Lee,⁴¹ S. W. Lee,⁴⁵ N. Leonardo,²⁷ S. Leone,³⁸ J. D. Lewis,¹³ K. Li,⁵² C. S. Lin,¹³ M. Lindgren,⁶ T. M. Liss,²⁰ J. B. Liu,⁴¹ T. Liu,¹³ Y. C. Liu,¹ D. O. Litvintsev,¹³ O. Lobban,⁴⁶ N. S. Lockyer,³⁷ A. Loginov,³⁰ J. Loken,³⁵ M. Loreti,³⁶ D. Lucchesi,³⁶ P. Lukens,¹³ S. Lusin,⁵¹ L. Lyons,³⁵ J. Lys,²⁵ R. Madrak,¹⁸ K. Maeshima,¹³ P. Maksimovic,²¹ L. Malferrari,³ M. Mangano,³⁸ G. Manca,³⁵ M. Mariotti,³⁶ G. Martignon,³⁶ M. Martin,²¹ A. Martin,⁵² V. Martin,³² M. Martínez,¹³ J. A. J. Matthews,³¹ P. Mazzanti,³ K. S. McFarland,⁴¹ P. McIntyre,⁴⁵ M. Menguzzato,³⁶ A. Menzione,³⁸ P. Merkel,¹³ C. Mesropian,⁴² A. Meyer,¹³ T. Miao,¹³ R. Miller,²⁹ J. S. Miller,²⁸ H. Minato,⁴⁸ S. Miscetti,¹⁵ M. Mishina,²³ G. Mitselmakher,¹⁴ Y. Miyazaki,³⁴ N. Moggi,³ E. Moore,³¹ R. Moore,²⁸ Y. Morita,²³ T. Moulik,⁴⁰ M. Mulhearn,²⁷ A. Mukherjee,¹³ T. Muller,²² A. Munar,³⁸ P. Murat,¹³ S. Murgia,²⁹ J. Nachtman,⁶ V. Nagaslaev,⁴⁶ S. Nahn,⁵² H. Nakada,⁴⁸ I. Nakano,¹⁹ R. Napora,²¹ F. Niell,²⁸ C. Nelson,¹³ T. Nelson,¹³ C. Neu,³³ M. S. Neubauer,²⁷ D. Neuberger,²² C. Newman-Holmes,¹³ C.-Y. P. Ngan,²⁷ T. Nigmanov,³⁹ H. Niu,⁴ L. Nodulman,² A. Nomerotski,¹⁴ S. H. Oh,¹² Y. D. Oh,²⁴ T. Ohmoto,¹⁹ T. Ohsugi,¹⁹ R. Oishi,⁴⁸ T. Okusawa,³⁴ J. Olsen,⁵¹ W. Orejudos,²⁵ C. Pagliarone,³⁸ F. Palmonari,³⁸ R. Paoletti,³⁸ V. Papadimitriou,⁴⁶ D. Partos,⁴ J. Patrick,¹³ G. Pauletta,⁴⁷ M. Paulini,⁹ T. Pauly,³⁵ C. Paus,²⁷ D. Pellett,⁵ A. Penzo,⁴⁷ L. Pescara,³⁶ T. J. Phillips,¹² G. Piacentino,³⁸ J. Piedra,⁸ K. T. Pitts,²⁰ A. Pompoš,⁴⁰ L. Pondrom,⁵¹ G. Pope,³⁹ T. Pratt,³⁵ F. Prokoshin,¹¹ J. Proudfoot,² F. Ptohos,¹⁵ O. Pukhov,¹¹

G. Punzi,³⁸ J. Rademacker,³⁵ A. Rakitine,²⁷ F. Ratnikov,⁴⁴ H. Ray,²⁸ D. Reher,²⁵ A. Reichold,³⁵ P. Renton,³⁵ M. Rescigno,⁴³ A. Ribon,³⁶ W. Riegler,¹⁸ F. Rimondi,³ L. Ristori,³⁸ W. J. Robertson,¹² T. Rodrigo,⁸ S. Rolli,⁴⁹ L. Rosenson,²⁷ R. Roser,¹³ R. Rossin,³⁶ C. Rott,⁴⁰ A. Roy,⁴⁰ A. Ruiz,⁸ D. Ryan,⁴⁹ A. Safonov,⁵ R. St. Denis,¹⁷ W. K. Sakumoto,⁴¹ D. Saltzberg,⁶ C. Sanchez,³³ A. Sansoni,¹⁵ L. Santi,⁴⁷ S. Sarkar,⁴³ H. Sato,⁴⁸ A. Savoy-Navarro,¹³ P. Schlabach,¹³ E. E. Schmidt,¹³ M. P. Schmidt,⁵² M. Schmitt,³² L. Scodellaro,³⁶ A. Scott,⁶ A. Scribano,³⁸ A. Sedov,⁴⁰ S. Seidel,³¹ Y. Seiya,⁴⁸ A. Semenov,¹¹ F. Semeria,³ T. Shah,²⁷ M. D. Shapiro,²⁵ P. F. Shepard,³⁹ T. Shibayama,⁴⁸ M. Shimojima,⁴⁸ M. Shochet,¹⁰ A. Sidoti,³⁶ J. Siegrist,²⁵ A. Sill,⁴⁶ P. Singh,²⁰ A. J. Slaughter,⁵² K. Sliwa,⁴⁹ F. D. Snider,¹³ R. Snihur,²⁶ A. Solodsky,⁴² J. Spalding,¹³ T. Speer,¹⁶ M. Spezziga,⁴⁶ P. Sphicas,²⁷ F. Spinella,³⁸ M. Spiropulu,¹⁰ L. Spiegel,¹³ J. Steele,⁵¹ A. Stefanini,³⁸ J. Strologas,²⁰ F. Strumia,¹⁶ D. Stuart,⁷ A. Sukhanov,¹⁴ K. Sumorok,²⁷ T. Suzuki,⁴⁸ T. Takano,³⁴ R. Takashima,¹⁹ K. Takikawa,⁴⁸ P. Tamburello,¹² M. Tanaka,⁴⁸ B. Tannenbaum,⁶ M. Tecchio,²⁸ R. J. Tesarek,¹³ P. K. Teng,¹ K. Terashi,⁴² S. Tether,²⁷ J. Thom,¹³ A. S. Thompson,¹⁷ E. Thomson,³³ R. Thurman-Keup,² P. Tipton,⁴¹ S. Tkaczyk,¹³ D. Toback,⁴⁵ K. Tollefson,²⁹ D. Tonelli,³⁸ M. Tonnesmann,²⁹ H. Toyoda,³⁴ J. F. de Troconiz,¹⁸ J. Tseng,²⁷ D. Tsybychev,¹⁴ N. Turini,³⁸ F. Ukegawa,⁴⁸ T. Unverhau,¹⁷ T. Vaicuiulis,⁴¹ J. Valls,⁴⁴ A. Varganov,²⁸ E. Vataga,³⁸ S. Vejcik III,¹³ G. Velev,¹³ G. Veramendi,²⁵ R. Vidal,¹³ I. Vila,⁸ R. Vilar,⁸ I. Volobouev,²⁵ M. von der Mey,⁶ D. Vucinic,²⁷ R. G. Wagner,² R. L. Wagner,¹³ W. Wagner,²² N. B. Wallace,⁴⁴ Z. Wan,⁴⁴ C. Wang,¹² M. J. Wang,¹ S. M. Wang,¹⁴ B. Ward,¹⁷ S. Waschke,¹⁷ T. Watanabe,⁴⁸ D. Waters,²⁶ T. Watts,⁴⁴ M. Weber,²⁵ H. Wenzel,²² W. C. Wester III,¹³ B. Whitehouse,⁴⁹ A. B. Wicklund,² E. Wicklund,¹³ T. Wilkes,⁵ H. H. Williams,³⁷ P. Wilson,¹³ B. L. Winer,³³ D. Winn,²⁸ S. Wolbers,¹³ D. Wolinski,²⁸ J. Wolinski,²⁹ S. Wolinski,²⁸ M. Wolter,⁴⁹ S. Worm,⁴⁴ X. Wu,¹⁶ F. Würthwein,²⁷ J. Wyss,³⁸ U. K. Yang,¹⁰ W. Yao,²⁵ G. P. Yeh,¹³ P. Yeh,¹ K. Yi,²¹ J. Yoh,¹³ C. Yosef,²⁹ T. Yoshida,³⁴ I. Yu,²⁴ S. Yu,³⁷ Z. Yu,⁵² J. C. Yun,¹³ L. Zanello,⁴³ A. Zanetti,⁴⁷ F. Zetti,²⁵ and S. Zucchelli³¹

(CDF Collaboration)

¹*Institute of Physics, Academia Sinica, Taipei, Taiwan 11529, Republic of China*²*Argonne National Laboratory, Argonne, Illinois 60439, USA*³*Istituto Nazionale di Fisica Nucleare, University of Bologna, I-40127 Bologna, Italy*⁴*Brandeis University, Waltham, Massachusetts 02254, USA*⁵*University of California at Davis, Davis, California 95616, USA*⁶*University of California at Los Angeles, Los Angeles, California 90024, USA*⁷*University of California at Santa Barbara, Santa Barbara, California 93106, USA*⁸*Instituto de Fisica de Cantabria, CSIC-University of Cantabria, 39005 Santander, Spain*⁹*Carnegie Mellon University, Pittsburgh, Pennsylvania 15213, USA*¹⁰*Enrico Fermi Institute, University of Chicago, Chicago, Illinois 60637, USA*¹¹*Joint Institute for Nuclear Research, RU-141980 Dubna, Russia*¹²*Duke University, Durham, North Carolina 27708, USA*¹³*Fermi National Accelerator Laboratory, Batavia, Illinois 60510, USA*¹⁴*University of Florida, Gainesville, Florida 32611, USA*¹⁵*Laboratori Nazionali di Frascati, Istituto Nazionale di Fisica Nucleare, I-00044 Frascati, Italy*¹⁶*University of Geneva, CH-1211 Geneva 4, Switzerland*¹⁷*Glasgow University, Glasgow G12 8QQ, United Kingdom*¹⁸*Harvard University, Cambridge, Massachusetts 02138, USA*¹⁹*Hiroshima University, Higashi-Hiroshima 724, Japan*²⁰*University of Illinois, Urbana, Illinois 61801, USA*²¹*The Johns Hopkins University, Baltimore, Maryland 21218, USA*²²*Institut für Experimentelle Kernphysik, Universität Karlsruhe, 76128 Karlsruhe, Germany*²³*High Energy Accelerator Research Organization (KEK), Tsukuba, Ibaraki 305, Japan*²⁴*Center for High Energy Physics, Kyungpook National University, Taegu 702-701, Korea; Seoul National University, Seoul 151-742, Korea; and Sung Kyun Kwan University, Suwon 440-746, Korea*²⁵*Ernest Orlando Lawrence Berkeley National Laboratory, Berkeley, California 94720, USA*²⁶*University College London, London WC1E 6BT, United Kingdom*²⁷*Massachusetts Institute of Technology, Cambridge, Massachusetts 02139, USA*²⁸*University of Michigan, Ann Arbor, Michigan 48109, USA*²⁹*Michigan State University, East Lansing, Michigan 48824, USA*³⁰*Institution for Theoretical and Experimental Physics, ITEP, Moscow 117259, Russia*³¹*University of New Mexico, Albuquerque, New Mexico 87131, USA*³²*Northwestern University, Evanston, Illinois 60208, USA*³³*The Ohio State University, Columbus, Ohio 43210, USA*

- ³⁴Osaka City University, Osaka 588, Japan
³⁵University of Oxford, Oxford OX1 3RH, United Kingdom
³⁶Universita di Padova, Istituto Nazionale di Fisica Nucleare, Sezione di Padova, I-35131 Padova, Italy
³⁷University of Pennsylvania, Philadelphia, Pennsylvania 19104, USA
³⁸Istituto Nazionale di Fisica Nucleare, University and Scuola Normale Superiore of Pisa, I-56100 Pisa, Italy
³⁹University of Pittsburgh, Pittsburgh, Pennsylvania 15260, USA
⁴⁰Purdue University, West Lafayette, Indiana 47907, USA
⁴¹University of Rochester, Rochester, New York 14627, USA
⁴²Rockefeller University, New York, New York 10021, USA
⁴³Istituto Nazionale de Fisica Nucleare, Sezione di Roma, University di Roma I, “La Sapienza,” I-00185 Roma, Italy
⁴⁴Rutgers University, Piscataway, New Jersey 08855, USA
⁴⁵Texas A&M University, College Station, Texas 77843, USA
⁴⁶Texas Tech University, Lubbock, Texas 79409, USA
⁴⁷Istituto Nazionale di Fisica Nucleare, University of Trieste, Udine, Italy
⁴⁸University of Tsukuba, Tsukuba, Ibaraki 305, Japan
⁴⁹Tufts University, Medford, Massachusetts 02155, USA
⁵⁰Waseda University, Tokyo 169, Japan
⁵¹University of Wisconsin, Madison, Wisconsin 53706, USA
⁵²Yale University, New Haven, Connecticut 06520, USA
(Received 15 February 2003; published 3 July 2003)

We report a measurement of the fraction of events with a large pseudorapidity gap $\Delta\eta$ within the pseudorapidity region available to the proton dissociation products X in $\bar{p} + p \rightarrow \bar{p} + X$. For a final state \bar{p} of fractional momentum loss $\xi_{\bar{p}}$ and 4-momentum transfer squared $t_{\bar{p}}$ within $0.06 < \xi_{\bar{p}} < 0.09$ and $|t_{\bar{p}}| < 1.0$ [0.2] GeV² at $\sqrt{s} = 1800$ [630] GeV, the fraction of events with $\Delta\eta > 3$ is found to be 0.246 ± 0.001 (stat) ± 0.042 (syst) [0.184 ± 0.001 (stat) ± 0.043 (syst)]. Our results are compared with gap fractions measured in minimum bias $\bar{p}p$ collisions and with theoretical expectations.

DOI: 10.1103/PhysRevLett.91.011802

PACS numbers: 13.85.Ni

In a previous Letter [1], we reported a measurement of the fraction of events with a central pseudorapidity gap $\Delta\eta$ [2] produced in $\bar{p}p$ collisions at $\sqrt{s} = 1800$ and 630 GeV. Here, we present results from a similar measurement performed in a subsample of $\bar{p}p$ events containing a leading (high longitudinal momentum) antiproton (Fig. 1). Large pseudorapidity gaps are presumed to be due to Pomeron (\mathbb{P}) exchange and are the signature for diffraction [3]. The process with a leading beam particle in the final state, which is kinematically associated with an adjacent pseudorapidity gap, is known as single diffraction dissociation (SD), while that with a central gap as double diffraction dissociation (DD). The process in Fig. 1 is a combination of \bar{p} - p SD and \mathbb{P} - p DD and will be referred to in this Letter as SDD.

Low transverse momentum (p_T) processes have traditionally been treated theoretically in the framework of Regge theory [3]. The introduction of a linear Pomeron (\mathbb{P}) trajectory, $\alpha(t) = \alpha(0) + \alpha' t$, with intercept $\alpha(0) = 1 + \epsilon > 1$, enables the theory to correctly predict certain salient features of the high energy behavior of hadronic interactions, such as the rise of the total cross section and the shrinking of the forward elastic scattering peak with increasing energy. However, the success of the theory in describing diffraction has been limited. While the shape of the SD and DD distributions as a function of $\Delta\eta$ are correctly described, the normalization was found to be suppressed relative to the theoretical predictions by about an order of magnitude as the energy increases from $\sqrt{s} \sim 20$ to 1800 GeV [1,4,5]. Proposals made to address this

issue are divided into two general groups: (a) those based on “damping” of the SD cross section at small (anti)proton fractional momentum loss ξ or on a changing Pomeron intercept as a function of \sqrt{s} [6] or as a function of ξ [7], and (b) those in which only the overall normalization is suppressed as \sqrt{s} increases [5,8–10]. The models of group (a) cannot be applied to SDD. In a parton model approach developed by Bjorken [11] to describe events with a large pseudorapidity gap between two jets produced by a colorless two-gluon exchange, a suppression of the overall normalization relative to the QCD calculation was predicted due to additional partonic *color* exchanges in the same event which spoil the diffractive pseudorapidity gap signature. In this model, which belongs to group (b), the color exchanges would simultaneously spoil all diffractive rapidity gaps in an event and therefore the ratio of two-gap to one-gap events in a given

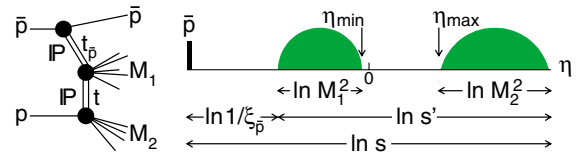


FIG. 1 (color online). Schematic diagram and event topology in pseudorapidity space of a SDD (single diffraction plus gap) interaction, $\bar{p} + p \rightarrow \bar{p} + \text{GAP}_{\bar{p}} + M_1 + \text{GAP} + M_2$, with a leading outgoing antiproton of fractional momentum loss $\xi_{\bar{p}}$, associated with a pseudorapidity gap $\Delta\eta_{\bar{p}} = \ln \frac{1}{\xi_{\bar{p}}}$, and a gap within the region of η spanned by $\ln s' = \ln s - \ln \frac{1}{\xi_{\bar{p}}}$.

interaction would be unaffected. This approach should also hold for low p_T diffractive processes. In this Letter, we examine this issue by studying $\bar{p} + p \rightarrow \bar{p} + X$ with/without a gap $\Delta\eta$ within the η range of the system X in addition to the gap of nominal [2] value $\Delta\eta_{\bar{p}} = -\ln\xi_{\bar{p}}$ expected to be associated with the leading final state antiproton.

Our study is based on our $\sqrt{s} = 1800$ (630) GeV inclusive SD data described in Ref. [12] ([13]). The events were collected in the 1995–1996 Tevatron Run 1C by triggering the Collider Detector at Fermilab (CDF) on an antiproton detected in a Roman Pot Spectrometer (RPS) [12]. The average instantaneous luminosity during event collection was 0.2×10^{30} (1.5×10^{30}) $\text{cm}^{-2} \text{sec}^{-1}$ at $\sqrt{s} = 1800$ (630) GeV. The components of CDF [14] relevant to this study are the central tracking chamber (CTC), the calorimeters, and two scintillation beam-beam counter (BBC) arrays. The CTC tracking efficiency varies from $\sim 60\%$ for $p_T = 300$ MeV to over 95% for $p_T > 400$ MeV within $|\eta| < 1.2$, and falls monotonically beyond $|\eta| = 1.2$ approaching zero at $|\eta| \sim 1.8$. The calorimeters have projective tower geometry and cover the regions $|\eta| < 1.1$ (central), $1.1 < |\eta| < 2.4$ (plug), and $2.2 < |\eta| < 4.2$ (forward). The $\Delta\eta \times \Delta\phi$ tower dimensions, where ϕ is the azimuthal angle, are approximately $0.1 \times 15^\circ$ for the central and $0.1 \times 5^\circ$ for the plug and forward calorimeters. The BBC arrays cover the region $3.2 < |\eta| < 5.9$.

The events were required to have a reconstructed RPS track of $0.06 < \xi_{\bar{p}} < 0.09$ and $|t_{\bar{p}}| < 1.0$ [0.2] GeV^2 at $\sqrt{s} = 1800$ [630] GeV, a hit on BBC_p (proton-side BBC) to exclude double Pomeron exchange events, and no more than one reconstructed vertex within ± 60 cm from the center of the detector along the beam direction. The vertex requirement was imposed to reject *overlap* events due to multiple interactions in the same beam-beam crossing, since additional interactions would most likely spoil the pseudorapidity gap signature of a diffractive event.

At $\sqrt{s} = 1800$ (630) GeV, the average $\xi_{\bar{p}}$ value of 0.075 of our data samples corresponds to \mathbb{P} - p collision energies of $\sqrt{s'} = \sqrt{\xi_{\bar{p}}s} = 493$ (173) GeV, at which the proton dissociation products cover the nominal η range from the maximum of $\eta = \ln\sqrt{s} = 7.5$ (6.5) down to $\eta = -\ln(\xi_{\bar{p}}\sqrt{s}) = -4.9$ (-3.9). Thus, the CDF calorimeter coverage, $|\eta| < 4.2$, is well suited for the present study.

Our analysis is similar to that used in evaluating the DD fraction in minimum bias events collected with a BBC coincidence trigger [1]. The method we use is based on the approximately flat dependence of the event rate on $\Delta\eta$ expected for SDD events compared to the exponential dependence expected for the normal SD events where rapidity gaps within the diffractive cluster X are due to random multiplicity fluctuations. Thus, in a plot of event rate versus $\Delta\eta$, the SDD signal will appear as a flattening of an exponentially falling distribution at large $\Delta\eta$ [11]. In order to independently monitor detector effects in the

positive and negative η directions, we look for η_{max} (η_{min}), the η of the particle closest to $\eta = 0$ in the proton (antiproton) direction, and measure *experimental* gaps overlapping $\eta = 0$, $\Delta\eta_{\text{exp}}^0 \equiv \eta_{\text{max}} - \eta_{\text{min}}$ (see Fig. 1). For this purpose, a particle is defined as a reconstructed track in the CTC, a calorimeter tower with energy above a given threshold, or a BBC hit. The tower energy thresholds used, chosen to lie comfortably above noise level, are $E_T = 0.2$ GeV for the central and plug and $E = 1$ GeV for the forward calorimeters. The calorimeter noise was measured using beam-beam crossing events with no reconstructed vertex. At the calorimeter interfaces near $|\eta| \sim 0, 1.1, \text{ and } \sim 2.4$, where the noise level was found to be higher, we use higher thresholds of up to 0.3 GeV. The average number of calorimeter towers per unit $\Delta\eta$ with E_T^{noise} above threshold in an event is ~ 0.07 , small compared to the corresponding average particle density of ~ 3 in the data. The fraction of SDD to total number of events based on $\Delta\eta_{\text{exp}}^0$ is obtained directly from the data and corrected for (a) contamination from SD events, (b) the effect of the unobserved (below threshold) particles, and (c) the triggering efficiency (acceptance) of BBC_p for SD and SDD events. These corrections are made using a hadron-level Monte Carlo (MC) simulation.

The MC generation of SD events is described in Ref. [4]. For SDD events, a diffractive \bar{p} and a cluster of $M_X^2 = s\xi$ are generated as for a SD interaction, and a DD interaction is assumed to take place in the \mathbb{P} - p collision, which is treated as in Ref. [1] and boosted to the lab frame. The same thresholds are used for particles in the MC as for towers in the data, after dividing the generated particle E_T by an η -dependent calibration coefficient of average value ~ 1.6 representing the ratio of true to measured calorimeter energy. The MC generator includes the calorimeter noise, and for charged particles it is followed by a detector simulation.

Figure 2 shows Lego histograms of events versus η_{max} and $-\eta_{\text{min}}$ for (a) data and (b) MC generated events, as well as MC events for (c) only SD and (d) only SDD at $\sqrt{s} = 1800$ GeV. Similar results are obtained at $\sqrt{s} = 630$ GeV. The observed structure in the distributions along $\eta_{\text{max}(\text{min})}$ is caused by the variation of the tower energy thresholds with $|\eta|$. The bins at $|\eta_{\text{max}(\text{min})}| = 3.3$ contain all events within the BBC range of $3.2 < |\eta_{\text{max}(\text{min})}| < 5.9$.

Figure 3 presents the number of events as a function of $\Delta\eta_{\text{exp}}^0$ for the 1800 GeV data (points) and for a fit to the data using a mixture of MC generated SD and SDD contributions (solid histogram). The SD contribution (dashed histogram) exhibits an approximately exponential fall with increasing $\Delta\eta_{\text{exp}}^0$, as expected. The region of $\Delta\eta_{\text{exp}}^0 > 3$ is dominated by the SDD signal and is used to extract the gap fraction (ratio of SDD to total number of events). The approximately flat behavior expected for the SDD distribution in this region is modulated by the η -dependent tower thresholds used, causing the observed bumps and dips, and by the BBC_p acceptance for SDD

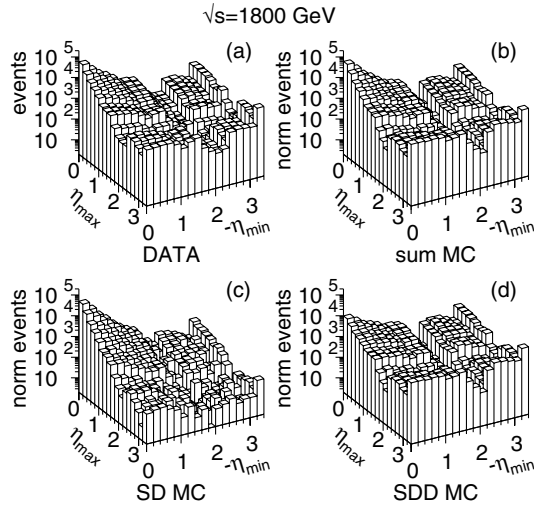


FIG. 2. The number of events as a function of η_{\max} and $-\eta_{\min}$, the η of the track or hit tower closest to $\eta = 0$ in the proton and antiproton direction, respectively, at $\sqrt{s} = 1800$ GeV: (a) data; (b) Monte Carlo simulation; (c),(d) the individual contributions of Monte Carlo generated SD and SDD (SD + gap) events. The MC distributions are normalized by a two-component fit to the data using distributions (c) and (d).

events, which decreases with increasing $\Delta\eta_{\text{exp}}^0$. The MC simulation reproduces these features of the data.

At $\sqrt{s} = 1800$ [630] GeV, the fraction of events with $\Delta\eta_{\text{exp}}^0 > 3$ is $(15.9 \pm 0.1)\%$ [$(17.5 \pm 0.2)\%$], of which the contribution of background SD events, estimated using the MC simulation, is 1.2% [2.4%]. The quoted errors are statistical. The amount of SD background in the region $\Delta\eta_{\text{exp}}^0 > 3$ depends on the tower energy calibration coefficients and thereby on the calorimeter tower energy thresholds used in the MC. For example, increasing these thresholds has the effect of decreasing the multiplicity in the MC generated events, resulting in larger rapidity gaps and hence larger SD background in the region of $\Delta\eta_{\text{exp}}^0 > 3$. The systematic uncertainty in the background is estimated by raising (lowering) the tower thresholds in the MC by a factor of 1.25 (evaluated from a multiplicity uncertainty of $\pm 10\%$), which increases (decreases) the background by a factor of 1.6.

The correction factors needed to account for the effect of unobserved particles and thus convert the measured gap fractions to gap fractions corresponding to the nominal gap definition [2], $\Delta\eta^0 \equiv \ln(s's_0/M_1^2 M_2^2)$

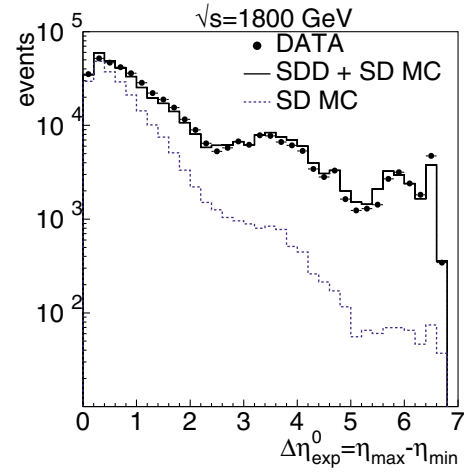


FIG. 3 (color online). The number of events as a function of $\Delta\eta_{\text{exp}}^0 = \eta_{\max} - \eta_{\min}$ for data at $\sqrt{s} = 1800$ GeV (points), for SD plus SDD (SD + gap) MC generated events (solid line), and for only SD MC events (dashed line).

[$\ln(M_i^2/\sqrt{s's_0}) < 0$, $i = 1, 2$], where $s_0 = 1 \text{ GeV}^2$, were evaluated using the SDD Monte Carlo simulation and found to be 0.81 [0.73] at $\sqrt{s} = 1800$ [630] GeV. Systematic errors are obtained by varying the tower energy thresholds by $\pm 25\%$. These errors are correlated with the errors in the SD background contamination and therefore a combined systematic uncertainty of 15% [23%] was evaluated for both these effects and applied to the extracted nominal gap fractions.

The BBC_p acceptance, evaluated from the SDD MC simulation, is $0.68 \pm 0.06(\text{syst})$ [$0.81 \pm 0.04(\text{syst})$], where the error is due to a 20% systematic uncertainty assigned to the fraction of the diffraction dissociation mass clusters which do not trigger the BBC_p . For SD events, the BBC acceptance is $0.98 \pm 0.01(\text{syst})$ [$0.98 \pm 0.01(\text{syst})$]. Including all systematic errors, the acceptance-corrected SDD fractions for nominal gaps $\Delta\eta^0 > 3$ are $0.174 \pm 0.001(\text{stat}) \pm 0.030(\text{syst})$ [$0.138 \pm 0.001(\text{stat}) \pm 0.032(\text{syst})$] at $\sqrt{s} = 1800$ [630] GeV.

The $\Delta\eta^0 > 3$ fractions are extrapolated to all SDD gaps of $\Delta\eta > 3$ using the shape of the gap distribution of Eq. (1), which is based on Regge theory and factorization. This equation, which was used in the MC simulation, is obtained from the equation for SD by replacing the \mathbb{P} - p total cross section factor with the \mathbb{P} - p DD factor $\kappa\{\cdot\cdot\}$ (see Ref. [1]).

$$\frac{d^5\sigma}{dt_{\bar{p}}dtd\xi_{\bar{p}}d\Delta\eta d\eta_c} = \left[\frac{\beta(t)}{4\sqrt{\pi}} e^{[\alpha(t_{\bar{p}})-1]\ln(1/\xi)} \right]^2 \times \kappa \left\{ \kappa \left[\frac{\beta(0)}{4\sqrt{\pi}} e^{[\alpha(t)-1]\Delta\eta} \right]^2 \kappa \left[\beta^2(0) \left(\frac{s''}{s_0} \right)^\epsilon \right] \right\}. \quad (1)$$

Here, η_c is the center of the gap $\Delta\eta$, $\beta(0)$ the \mathbb{P} - p coupling, κ the ratio of the triple-Pomeron to the \mathbb{P} - p couplings, and $\ln \frac{s''}{s_0} = \ln \frac{s}{s_0} - \ln \frac{1}{\xi_{\bar{p}}} - \Delta\eta$ the rapidity space occupied by particles; $\sqrt{s''}$ will be referred to below as “diffractive subenergy.” For numerical evaluations we use [1] $\epsilon = 0.104 \pm 0.002$, $\alpha' = 0.25 \text{ GeV}^{-2}$, $\kappa = 0.17$,

$\beta(t_{\bar{p}}) = 6.57 \text{ GeV}^{-1}$ [$4.1 \text{ mb}^{1/2}$] $\times F_1(t_{\bar{p}})$, where $F_1(t_{\bar{p}})$ is the nucleon form factor. The variable t is not measured and therefore is integrated over in the calculations. Owing to the increased phase space resulting from releasing the requirement that the rapidity gap overlap $\eta = 0$, the

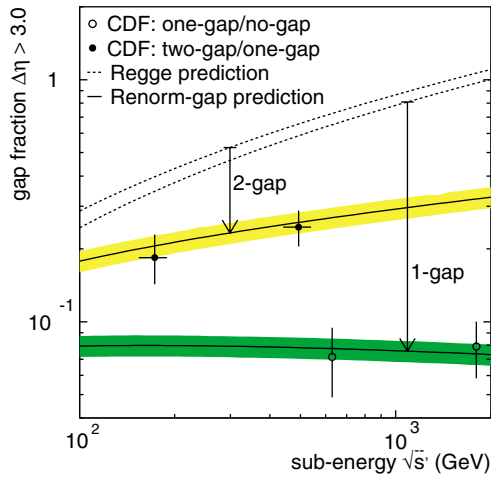


FIG. 4 (color online). Ratios of SDD (single-diffraction plus gap) to single-diffractive rates (solid circles) and double-diffractive to total cross sections (open circles) as a function of the collision energy of the subprocess, Pomeron-proton, and $\bar{p}p$, respectively. The uncertainties are mainly due to systematic effects, which are highly correlated among all four data points. The dashed lines are predictions from Regge theory and the solid lines from the renormalized gap probability model [10].

$\Delta\eta > 3$ fractions are found to be larger than the $\Delta\eta^0 > 3$ ones by a factor of 1.44 [1.40] at $\sqrt{s} = 1800$ [630] GeV. The evaluation of this factor is performed analytically and therefore no error is assigned to it; the effect of the uncertainty in the parameter ϵ , which controls the shape of the $\Delta\eta$ distribution in Eq. (1), is $< 1\%$.

Our results for the ratio R_{SD}^{SDD} of the number of events with a gap of $\Delta\eta > 3$ to the total number of SD events are 0.246 ± 0.001 (stat) ± 0.042 (syst) [0.184 ± 0.001 (stat) ± 0.043 (syst)] at $\sqrt{s} = 1800$ [630] GeV. These ratios are plotted in Fig. 4 at $\sqrt{s'} = 493$ [173] GeV, the average value of the diffractive mass M_X , and compared with double-diffractive to total cross section ratios $R_T^{DD} = \sigma^{DD}/\sigma_T$, where σ^{DD} is obtained from [1] and σ_T is set to the Pomeron exchange contribution, $\beta^2(0)(\frac{s}{s_0})^\epsilon$, to conform with the definition of R_{SD}^{SDD} . The vertical error bars are mainly due to systematic effects, which are correlated among all points. The dashed lines represent predictions based on Regge theory and factorization normalized to the SD cross section at $\sqrt{s} = 22$ GeV (see [10]). The solid lines are predictions from the “renormalized gap probability” model [10], in which the Regge cross section is factorized into two parts, one representing the $\bar{p}p$ total cross section at the diffractive subenergy multiplied by κ^n , where n is the number of gaps, and a factor interpreted as the gap probability distribution normalized to unity over all available phase space. The bands around the solid lines represent a 10% uncertainty due to the factor κ [15]. The data are in good agreement with the renormalized gap model predictions.

In summary, we have measured the fraction of events with a pseudorapidity gap $\Delta\eta > 3$ within the diffractive cluster X of the process $\bar{p}p \rightarrow \bar{p}X$ and found it to be 0.246 ± 0.001 (stat) ± 0.042 (syst) [0.184 ± 0.001 (stat) ± 0.043 (syst)] for $0.06 < \xi_{\bar{p}} < 0.09$ and $|t_{\bar{p}}| < 1.0$ [0.2] GeV² at $\sqrt{s} = 1800$ [630] GeV. These values are higher than expectations from double-diffractive fractions in minimum bias events, lower than expectations from Regge theory and factorization, and in good agreement with predictions based on the renormalized gap probability model [10].

We thank the Fermilab staff and the technical staffs of the participating institutions for their vital contributions. This work was supported by the U.S. Department of Energy and National Science Foundation; the Italian Istituto Nazionale di Fisica Nucleare; the Ministry of Education, Culture, Sports, Science and Technology of Japan; the Natural Sciences and Engineering Research Council of Canada; the National Science Council of the Republic of China; the Swiss National Science Foundation; the A. P. Sloan Foundation; the Bundesministerium fuer Bildung und Forschung, Germany; and the Korea Science and Engineering Foundation.

- [1] T. Affolder *et al.*, Phys. Rev. Lett. **87**, 141802 (2001).
- [2] Pseudorapidity gap is a region of pseudorapidity η devoid of particles; $\eta \equiv -\text{Intan}\frac{\theta}{2}$, where θ is the polar angle relative to the proton beam direction. The term *nominal* η is used to refer to the η of a particle of momentum p assuming $p_T = 1$ GeV/ c .
- [3] P. D. B. Collins, *An Introduction to Regge Theory and High Energy Physics* (Cambridge University Press, Cambridge, United Kingdom, 1977); V. Barone and E. Predazzi, *High-Energy Particle Diffraction* (Springer Press, New York, 2001).
- [4] F. Abe *et al.*, Phys. Rev. D **50**, 5535 (1994); **50**, 5550 (1994).
- [5] K. Goulianos, Phys. Lett. B **358**, 379 (1995).
- [6] S. Erhan and P. Schlein, Phys. Lett. B **427**, 389 (1998); **481**, 177 (2000).
- [7] Chung-I Tan, Phys. Rep. **315**, 175 (1999).
- [8] A. Kaidalov, in *Proceedings of VIIth Blois Workshop on Elastic and Diffractive Scattering, Château de Blois, France, 1995*, edited by P. Chiappetta, M. Haguenaer, and J. Trân Thanh Vân (Editions Frontières, Gif-sur-Cedex, France, 1996), pp. 107–115.
- [9] See E. Gotsman, E. M. Levin, and U. Maor, Phys. Rev. D **60**, 094011 (1999).
- [10] K. Goulianos, hep-ph/0203141.
- [11] J. D. Bjorken, Phys. Rev. D **47**, 101 (1993).
- [12] T. Affolder *et al.*, Phys. Rev. Lett. **84**, 5043 (2000).
- [13] D. Acosta *et al.*, Phys. Rev. Lett. **88**, 151802 (2002).
- [14] F. Abe *et al.*, Nucl. Instrum. Methods Phys. Res., Sect. A **271**, 387 (1988).
- [15] K. Goulianos and J. Montanha, Phys. Rev. D **59**, 114017 (1999).